https://dx.doi.org/10.22161/ijaers/3.10.31 *ISSN: 2349-6495(P) | 2456-1908(O)*

Impact of the Nozzle Angles on Counterflow Diffusion Flame to Strain Rate Variations

Assist. Prof. Dr. Jassim M. Abdulkarim [1], Prof. Dr. Jamal Y. Al Abass[2] , Paiman S. Salih[3], Shadi B. Ahmed [4], Hanin N. Al-Kalany[5]

[1,3,4]Department of Production Engineering & Metallurgy, Sulaimani Polytechnic University, Sulaimani–Iraq
[2,5]Department of Engineering - Damascus University, Syria

Abstract*—The Diffusion laminar combustion of liquefied petroleum gas (LPG) and air is studied experimentally using counterflowing axisymmetric jets. Attributes of this type of burner arrangement for studying laminar combustion are discussed in terms of flame geometry, angle of nozzle, strain rate, and measurement access.*

In the current research, an integrated combustion system was designed and developed for a type of counterflow diffusion flame. To study formation of the disc flame and the limits of stability, three types of nozzle with different angles (30°, 45°, and 60°) were used, an integrated design of two perpendicular burners was made to maintain the temperature of the mixture constant before the reaction. In the current study the charts of flame stability of diffusion flame with different equivalence ratios ($0.65 \leq \phi \geq 1.45$) are obtained , and determine the limits of temperature distribution and strain rate.

Keywords*— *Diffusion Counter flame, strain rate, and Flame Extinction.

I. INTRODUCTION

Information of extinction limits of laminar flames under periodic strain is required to quantify the influence of length and time scales of flame quenching and to assist modeling of flame extinction. In this context, unforced flame extinction has been examined theoretically, for example by [1] in laminar counterflow flames and[2] in turbulent counterflow flames, but forced flame extinction has received limited attention in spite of its importance to practical devices, such as gas turbine combustors, IC and air craft engines[3]. The optimization of practical combustion devices requires a detailed knowledge of the combustion kinetic.

Moreover, most practical combustion systems operate at pressures well above (0.1MPa) (gas turbines, aeronautic turbines, engines). The development and validation of detailed combustion mechanisms must therefore take into account the influence of temperature flame front. Most of the combustion kinetic mechanisms have been validated in nozzle (burner) laboratory conditions (flow, homogeneous reactors, and nonpremixed flames).

1.1 Parabolic Profile at Nozzles Exit

The assumption of fully-developed parabolic flow field at the nozzles exit was first examined by[4,5]. The entrance length EL figure 1 is the length of the tube necessary to have a fully developed parabolic profile. It is a function of many parameters, such as Reynolds number, flow condition at the tube inlet, temperature gradients, tube surface, etc. In the literature [6], an approximate value is assumed to be:

$EL = L/d = 0.6\ Re$ (Laminar flow) (1)

$EL = L/d = 4.4\ Re^{1/6}$ (Turbulent flow) (2)

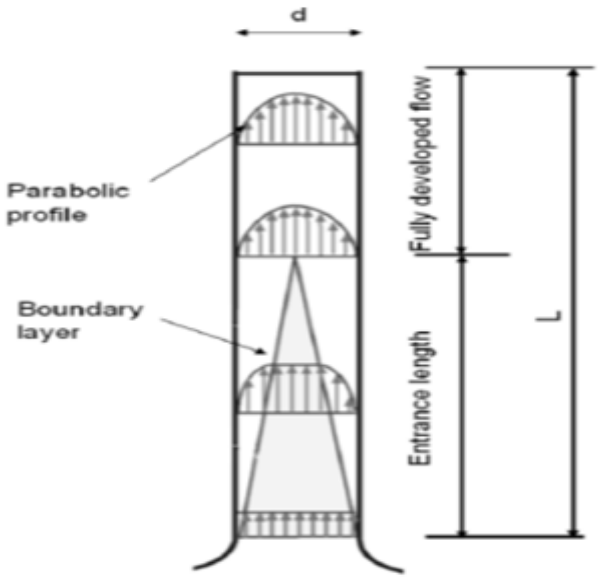

Fig.1: Schematic of the entrance length in a tube[6].

1.2 The Mixing Rate

The effect of mixing in laminar flames is usually quantified by the local strain rate of the flame. In turbulent sooting flames, however, the evaluation of the strain rate is predominantly based on global characteristics, rather than on local values, due to the difficulties of undertaking such measurements in unsteady flames. However, similar trends as in laminar flames are observed. Investigations performed by[7] in a simple turbulent jet flame have shown that the average soot volume fraction decreases with increasing characteristic

https://dx.doi.org/10.22161/ijaers/3.10.31 *ISSN: 2349-6495(P) | 2456-1908(O)*

strain rate. In addition, the rate of this decrease is higher at high mixing rates than at low mixing rates. Later measurements by[8] revealed an inverse relationship between global mixing rates and the total volume fraction of soot. Laminar diffusion flames can be investigated to obtain detailed explanations on these types of observations. An illustration of soot formation in a non-premixed counterflow diffusion flame is shown in Figure 2 The soot precursors and young soot particles are generated close to the stoichiometric plane. Surface growth reactions and particle coagulation take place during the time of convective transport from the flame surface toward the stagnation plane. Hence, the residence time of the sooting gas particles depends on the applied strain and the axial co-ordinate.

Of particular significance is the finding that the scalar structure of these flames are largely insensitive to strain rate variations, even near the state of extinction. For mixtures that are basically diffusionally neutral[9], the scalar structure can be considered to be basically invariant to the imposed strain rate. For mixtures which are diffusionally imbalanced, such as the lean and rich methane/air and propane/air mixtures, the insensitivity of the scalar structure especially its thickness is still quite substantial, although differences are noticeable.

It can be observed that for the given alkanes (CH_4 and C_3H_8), the effect of the strain rate is of about two to three orders stronger compared to the ethylene-flame. However, this sensitivity is not necessarily true in all circumstances (e.g., for all fuel types). In particular, when using more practical fuel types consisting of larger aromatic compounds, the inception path can be drastically different than the ones proposed for ethylene[10].

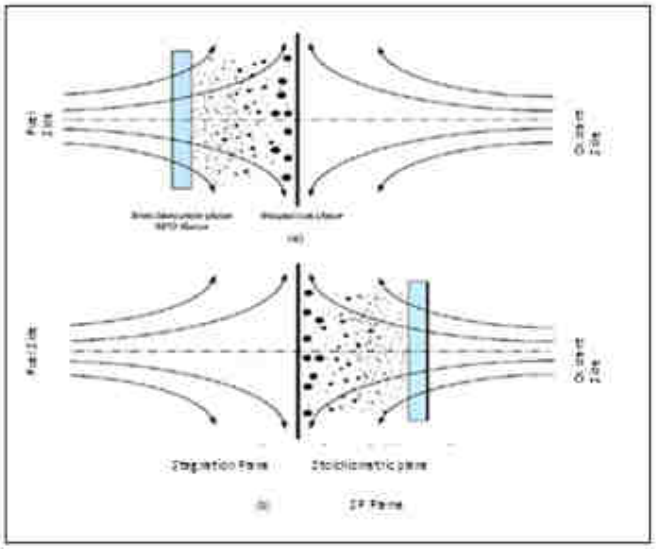

Fig. 2: Illustration of PAH / soot formation in SF (top) and SFO (bottom) counterflow flames[10].

II. MATHEMATICAL FORMULATION

In figure 3 we show a schematic illustration of a counterflow diffusion flame stabilized near the stagnation plane of two steady, laminar, infinitely wide, axisymmetric, counterflowing, reactant jets. If we let x and y denote the independent spatial coordinates in the tangential and the transverse directions, respectively, then the oxidizer jet is located at y = ∞ and the fuel jet at y = -∞. For large values of the Damkohler number, chemical reaction occurs predominantly in a thin zone near the plane where the fluxes of the fuel and the oxidizer flow in stoichiometric proportion. The structure of the flame can be obtained as the solution of a set of coupled nonlinear two-point boundary value problems along the stagnation streamline. Our model assumes the flow to be laminar, stagnation point flow in cylindrical coordinates. The governing boundary layer equations for mass, momentum, chemical species and energy can be written in the form:

$$\frac{\partial(\rho u x)}{\partial x} + \frac{\partial(\rho v x)}{\partial y} = 0 \qquad (3)$$

$$\rho u \frac{\partial u}{\partial x} + \rho v \frac{\partial u}{\partial y} + \frac{\partial P}{\partial x} = \frac{\partial}{\partial y}\left(\mu \frac{\partial u}{\partial y}\right) \qquad (4)$$

$$\rho u \frac{\partial Y_k}{\partial x} + \rho v \frac{\partial Y_k}{\partial y} + \frac{\partial}{\partial y}\left(\rho Y_k V_{ky}\right) - \dot{w}_k W_k = 0$$

$$k = 1,2,\ldots,k, \qquad (5)$$

$$\rho u c_p \frac{\partial T}{\partial x} + \rho v c_p \frac{\partial T}{\partial y} - \frac{\partial}{\partial y}\left(\lambda \frac{\partial T}{\partial Y}\right) +$$

$$\sum_{k=1}^{k} \rho Y_k V_{ky} c_{pk} \frac{\partial T}{\partial y} + \sum_{k=1}^{k} \dot{w}_k W_k h_k = 0 \qquad (6)$$

The system is closed with the ideal gas law,

$$\rho \frac{p\bar{W}}{RT} \qquad (7)$$

The system is made dimensionless, the reference temperature is $\frac{\tilde{q}}{Cp}$.

Where:

$$\tilde{q} = \frac{\tilde{Q}\tilde{X}_{F,L}}{V_f W_f} \qquad (8)$$

represents the heat released pure unit mass of fuel consumed. In these equations T, denotes the temperature; Y_k, the mass fraction of the k^{th} species; p, the pressure; u and v the tangential .and the transverse components of the

https://dx.doi.org/10.22161/ijaers/3.10.31 *ISSN: 2349-6495(P) | 2456-1908(O)*

velocity, respectively; ρ, the mass density; W_k, the molecular weight of the k^{th} species; $\bar{W}$, the mean molecular weight of the mixture; R, the universal gas constant; λ, the thermal conductivity of the mixture; c_p, the constant pressure heat capacity of the mixture; c_{pk}, the constant pressure heat capacity of the k^{th} species; $\dot{w}_k$, the molar rate of production of the k^{th} species per unit volume; h_k, the specific enthalpy of the k^{th} species; μ the viscosity of the mixture and V_{ky} is the diffusion velocity of the k^{th} species in the y direction. The form of the chemical production rates and the diffusion velocities can be found in detail in Refs.[11,12]. The free stream tangential and transverse velocities at the edge of the boundary layer are given by u_∞ = ax and vx = - 2_{ay} where a is the strain rate.

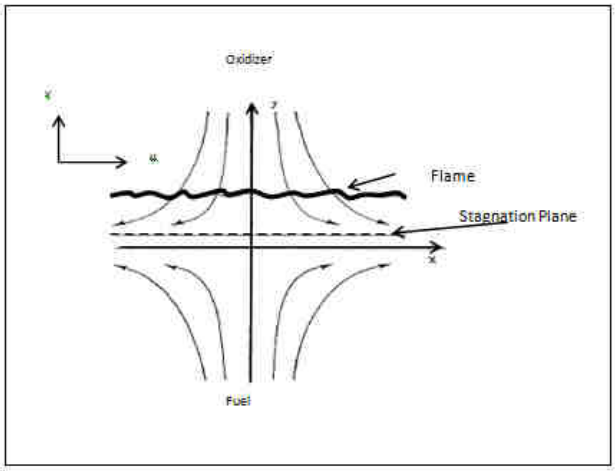

Fig. 3: Schematic illustration of a counterflow flame.

III. EXPERIMENTAL SETUP

3.1 Counterflow Apparatus

The counterflow apparatus consisted of two convergent nozzle burners with (12 mm) exit diameters vertically opposed brass tubes and were spaced (20 mm) apart. Outer thermal class box (20, 20, 20) cm, were used to isolate and stabilize the double flame in order to use three angles of nozzle (30, 45, 60 deg.) to compare the experimental data, figure 4 gives the schematic of the counterflow nozzle burner. The improvement of data accuracy of measurement will be discussed later.

Consequently, the fuel (LPG) and oxidizer (air) streams respectively consisted of different equivalence ratio ($0.65 \leq \phi \leq 1.48$). In addition, the mean exit velocities at the nozzles were kept equal.

The fuel was LPG of approximate composition (40% C_3H_8, 60 % C_4H_{10}), drawn from the mains by a compressor at a pressure of (1 bars) (gauge), and filtered to remove the dust particles, oil, and water droplets with diameters greater than 2μm.Flow rates were metered by flowmeters calibrated by the manufactures and arranged, so that each burner could be supplied with (0-16 L/min) air and (0-6 L/min) of gas for diffusion flames. The moment of the two jets was kept equal, so that the stagnation plane of the nonoscillating flow was located at the half distance, H/2, between the two opposing assemblies. Figure 5 gives the schematic diagram of the experimental test rig, and the photo is shown in figure 6.

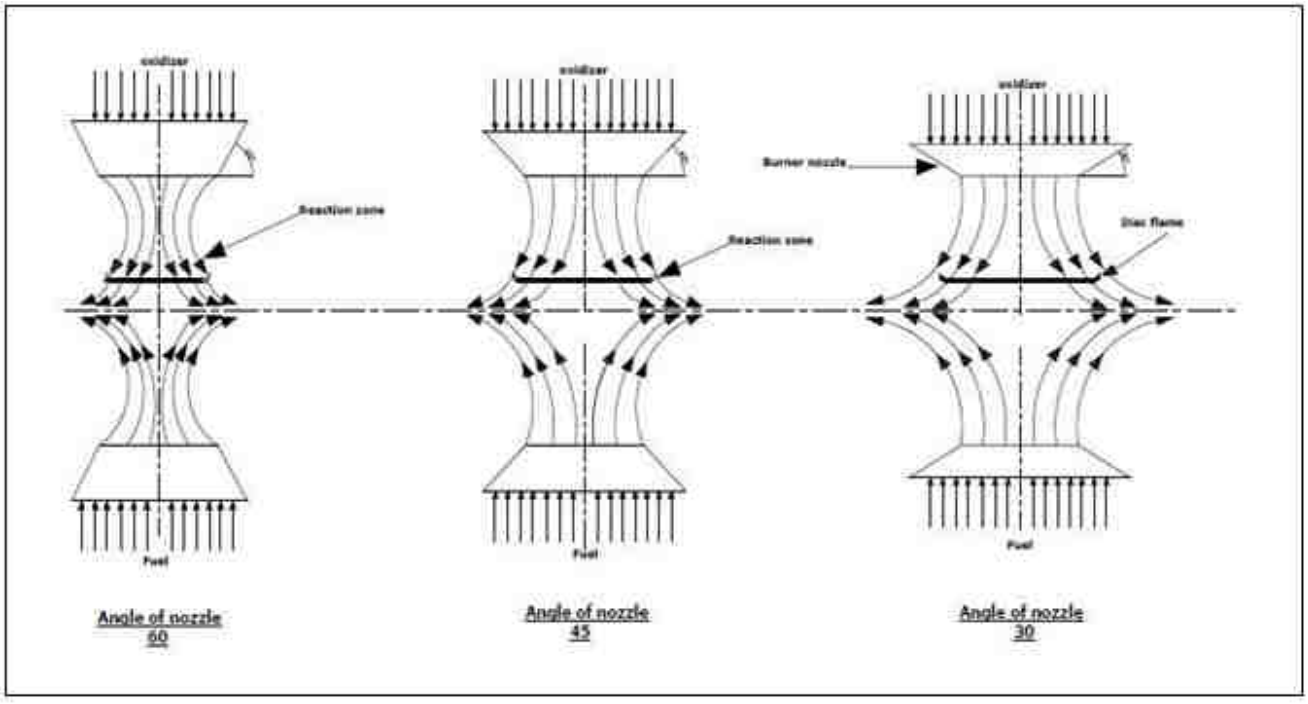

Fig. 4: Schematic illustration of the counterflow nozzle burner.

https://dx.doi.org/10.22161/ijaers/3.10.31 *ISSN: 2349-6495(P) | 2456-1908(O)*

Nonpremixed and partially premixed flames were better characterized by the air volume fraction in the fuel stream, X, defined as:

$$X = \frac{\dot{Q}air}{(\dot{Q}fuel + \dot{Q}air)} \quad (9)$$

Luminous photographs of the evolution of a vortex during one period of oscillation were obtained to characterize the instantaneous flow field under periodic forcing and to provide correlations between the temporal evolution of the vortex rings and flame extinction. Initial experiments with inert and combusting counterflows confirmed that the evolution of a vortex during one period of oscillation was similar for both arrangements.

Extinction of the nonoscillating flames was measured by increasing the fuel flow ($\dot{Q}fuel$) to a rate of (0.5 L/min) and simultaneously adjusting the air flow in the two streams so that the equivalence ratio remained constant as the bulk velocity and strain rate were increased. The bulk velocities, Ub_{ext}, at which extinction occurred were the average of three measurements with an estimated uncertainty less than 10%, and the respective extinction bulk strain rates were calculated from[13].

$$Sb_{ext} = \frac{U_{b_{ext}}}{(H/2)} \quad (10)$$

Extinction of the oscillating flames was measured in terms of the time elapsed from the beginning of an impulsively applied oscillation until extinction. An unforced flame was first arranged by adjusting the fuel and air flowrates so that the bulk velocities were lower than the unforced extinction limits.

The motivation for this choice was to examine the flame response to periodic straining and, in parallel, to quantify the extinction time scales of flames near the extinction limits, as can be the case in gas turbine combustors with lean mixtures and self-induced oscillations. It is also demonstrated that periodically forced flames, even close to their unforced extinction limits, can withstand velocity fluctuations of the order of the bulk velocity provided the time of pulsation does not exceed a critical timescale.

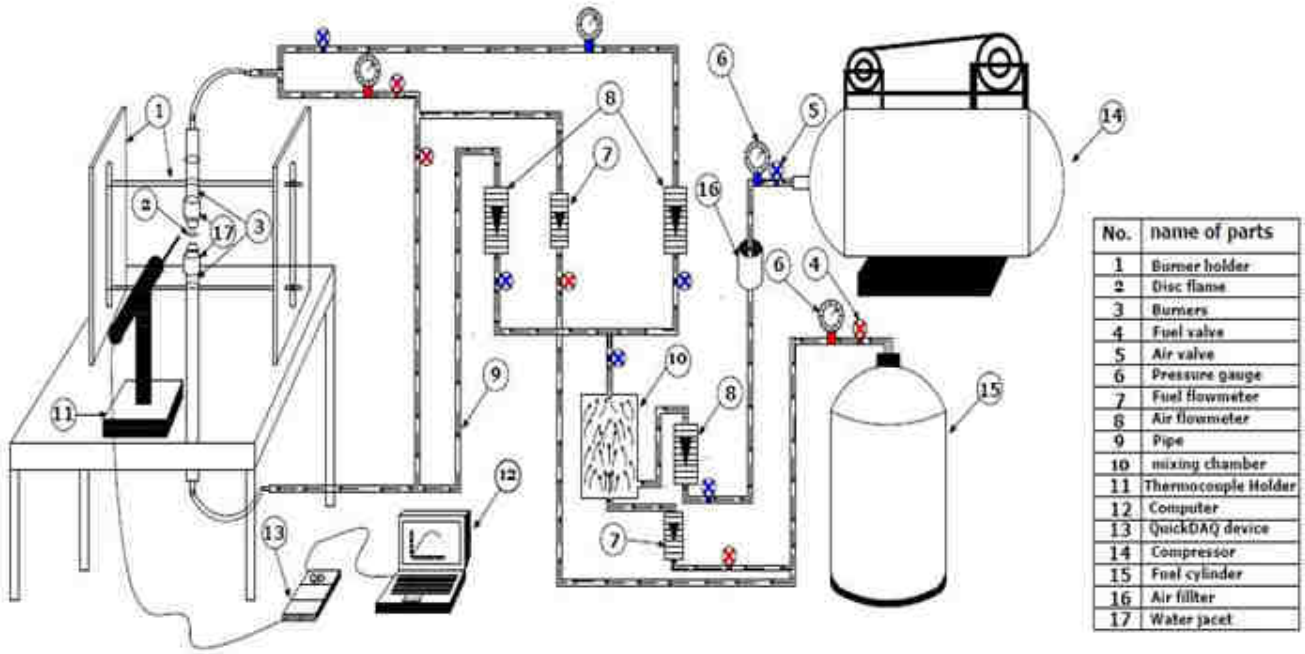

No.	name of parts
1	Burner holder
2	Disc flame
3	Burners
4	Fuel valve
5	Air valve
6	Pressure gauge
7	Fuel flowmeter
8	Air flowmeter
9	Pipe
10	mixing chamber
11	Thermocouple Holder
12	Computer
13	QuickDAQ device
14	Compressor
15	Fuel cylinder
16	Air fillter
17	Water jacet

Fig. 5: Schematic diagram of the experimental test rig.

https://dx.doi.org/10.22161/ijaers/3.10.31 ISSN: 2349-6495(P) | 2456-1908(O)

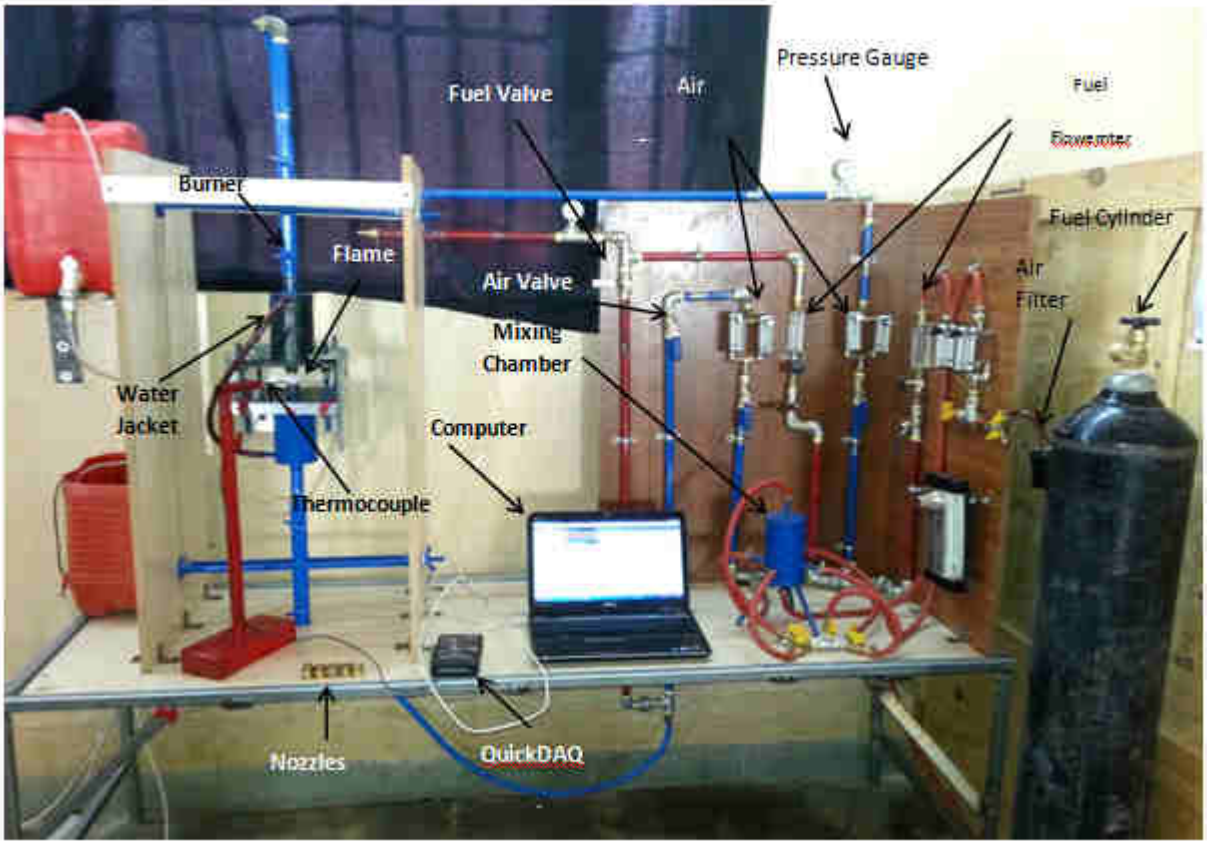

Fig. 6: Photograph of the counterflow burner facility[14].

3.2 Burner Characterization

Mixture composition profiles taken between the two injections were used to define the injection layer thickness, the effective boundary conditions and the mixture strength.

The contoured design of flow nozzle, coupled to $(1/25)^{th}$ cell size honeycombs, guarantees an exit velocity profile with reasonable uniformity. Contained several fine wire mesh screens near the nozzle exits, a standard technique causing the flow to be laminar[15,16,17]. The same burner can be used under diffusion and partially premixed conditions. In such a case, two identical premixed streams are fed to top and bottom burner, and twin flames are established symmetrically with respect to the gas stagnation plane. The exit conditions were standard temperature and atmospheric pressure. The injection Reynolds number, based on the velocity of the mixture during the injection interval, the cold mixture viscosity and the exit nozzle diameter, was between $861.11 \leq Re_{jet} \leq 1377.78$. The burners were cooled using a closed loop water circulation at a fixed temperature between (30 and 35 ^{O}C) depending on the flame conditions and to avoid water condensation at the burner surfaces, figure 7 shows the details of burners.

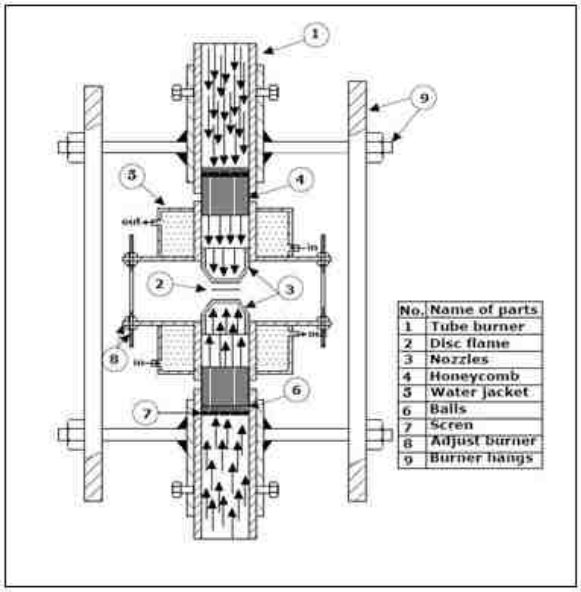

Fig. 7: details of burners.

IV. RESULTS AND DISCUSSION

4.1 Limits of Operation (Flame Position)

To measure the flame location in the burner, photographs were taken from the side. The images were then analyzed, and the flame position was determined as the point of maximum luminosity in the center between the burners. This optically determined flame location was checked to

https://dx.doi.org/10.22161/ijaers/3.10.31 *ISSN: 2349-6495(P) | 2456-1908(O)*

be in excellent agreement with the location of temperature maximum. The flames were stabilized about the point where the mean velocity of propagation equals the mean axial flow velocity of the reactants. The flame surfaces appeared undulatory and rapidly changing about this stable mean position. The effects of buoyancy were more pronounced in making the flow asymmetric at lower flow velocities and large nozzle separation.

For each experimental condition, the effective mixture composition immediately next to the injection needle array supplying the counter-diffusing species was measured by mass spectrometry. These local concentration profiles, extending from the injection tube tips to the flame, allowed the determination of the effective boundary condition at the edge of the downstream injection layer, i.e., the amount of reactant swept into the exhaust by the bulk flow, and hence the effective mixture strength in the burner. Based on this concentration profile, a point beyond the injection layer was chosen as the virtual origin of the counter-diffusing reactant. The mixture composition and temperature at this point were then used as boundary condition and the reduced chamber length as the new reference length for the comparison with the simplified model. This procedure allowed the effective mixture strength / to be kept constant, despite the varying loss of counter-diffusing species into the exhaust at different bulk flow velocities.

Figure 8. shows the types of diffusion flame stability at different equivalent ratio, and figure 9. shows the flame fronts with the change of the fuel direction.

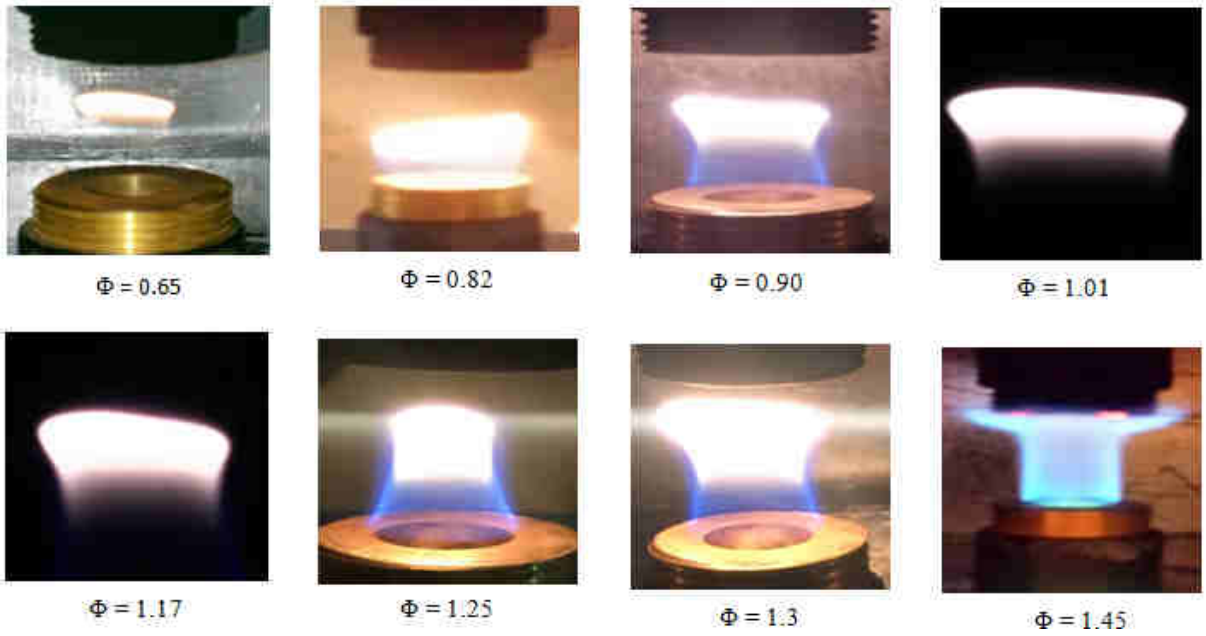

Fig. 8: Counter diffusion flames with different equivalence ratio (Φ).

Fig. 9: Types of diffusion flames.

Figure 10 shows the stability limits of diffusion flame front, where the blue area dimly represents the lean diffusion flame disc so as to increase the air ratio of the allowable limit, as for red area which represents the rich flame disc, this is due to increase in fuel ratio, while the blue line dark that divided the two regions represents a diffusion flame zone at stoichiometric air to fuel ratio, and any area outside those areas indicates instability and

https://dx.doi.org/10.22161/ijaers/3.10.31 *ISSN: 2349-6495(P) | 2456-1908(O)*

quenching of the flames due to the disproportion amount of mixing fuel and air and the difficulty of mixing between them, which is lead to not completeness of ideal combustion and instability of the flame and its extinguishment.

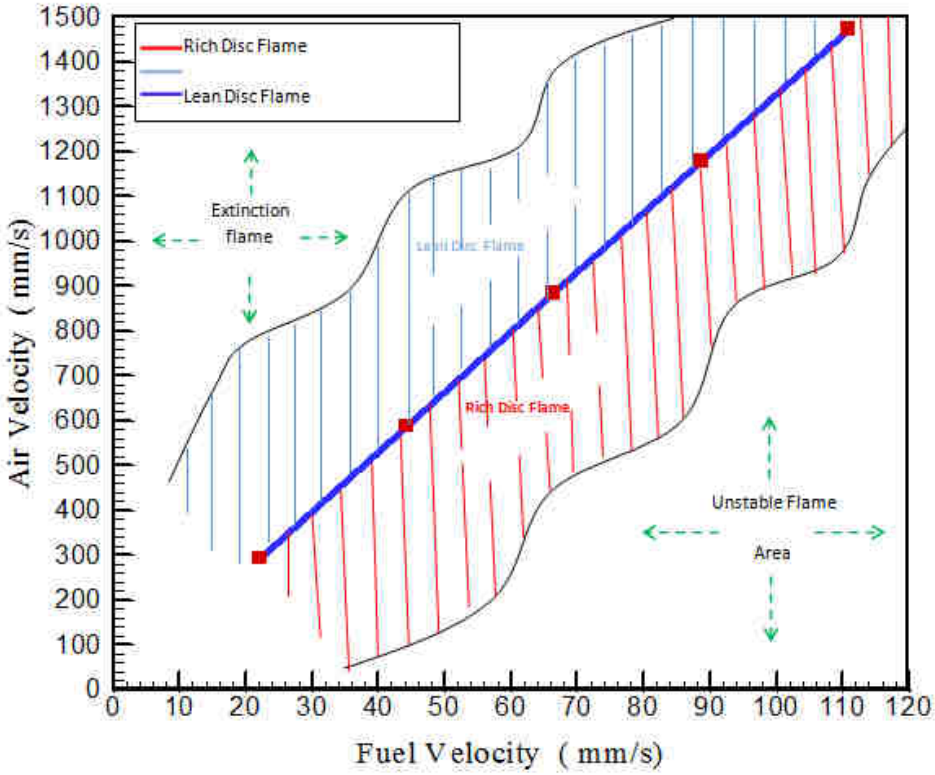

Fig. 10: Limits of operation (Flame Position).

4.2 Unforced Flame Extinction

The underlying chemical mechanism of transient flame extinction under periodic forcing can be understood better by consideration of the laminar flamelet calculations of[18]. These reveal that the rate of the main branching reaction, $H + O_2 = OH + H$, gradually decreases when the periodic strain exceeds the unforced extinction value, with consequent reactant leakage through the reaction zone, accumulation of substantial amounts of O_2, and decrease in the maximum temperature. If the flame experiences favorable straining before it reaches permanent extinction, the reaction resumes provided the temperature in the reaction zone is sufficiently high, and the H radicals in the reaction zone are not disproportionately depleted. However, the reduced fuel consumption in the local quenching and reignition stages limits the overall supply of H radicals, leading to a gradual reduction of the H radical pool. Thus extinction may be initiated by strain but will not be completed unless the time of the oscillation is sufficient to allow complete shutdown of chemical processes.

So that results obtained in an unforced counterflow must be representative of other configurations characterized by short residence times, and Sardi and Taylor[19] showed this to be true in the vicinity of the exit of a turbulent jet, which is the critical region for the stabilization of a nonpremixed flame. As a consequence, the local equivalence ratio of the reactants is altered and this is in agreement with the theoretical investigations of Karagozian and Marble[20] who suggest that vortices enhance molecular mixing. Figure 11 shows the relationship between air volume fraction on the fuel stream (X) and extinction velocity by changing of jet angles, which indicate that wherever there is a decrease in fuel and oxidized flow path angle there is an increase in limits of the stability of the flame as well as the strain rate. The reason is due to increase in aerodynamic diffuse between the reactants and heat and mass transfer that influenced by the direction of the jet angle which is due to formation of the recirculation area between the reactants therefore determine the amount and efficiency of mixing and diffuse air to the fuel.

https://dx.doi.org/10.22161/ijaers/3.10.31 *ISSN: 2349-6495(P) | 2456-1908(O)*

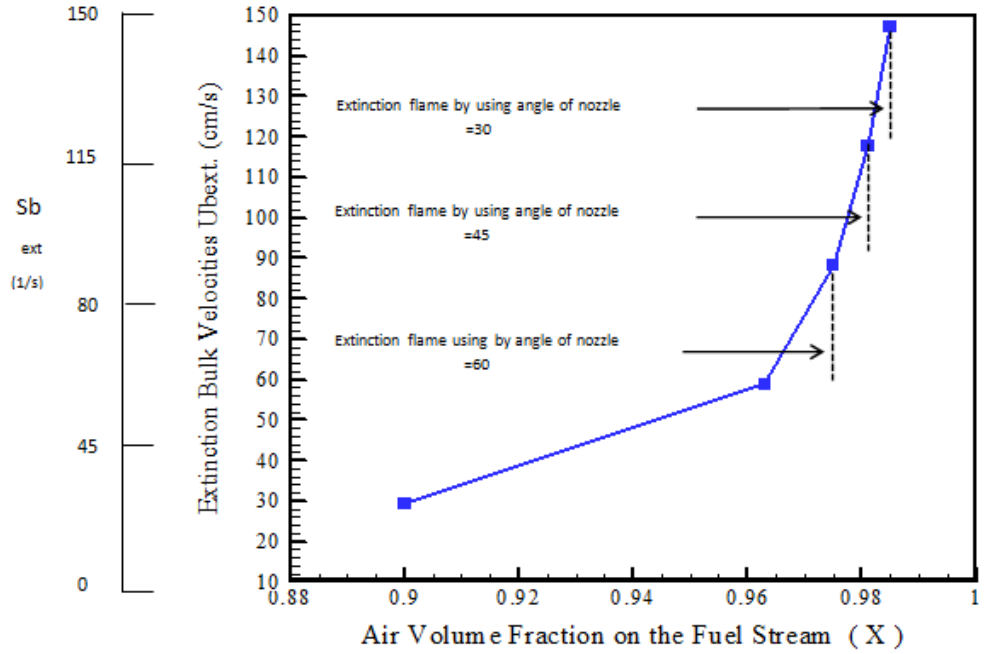

Fig. 11: Extinction bulk Velocities Ub_{ext}, and bulk strain rates Sb_{ext} in (1/s), of counter diffusion flame

4.3 Flame Temperature

The design of the combustion chambers and industrial furnaces depends on the shape of the temperature distribution and the diameter of flame front. As a result, temperature and composition profile were measured near the stagnation stream line along a coordinate normal to the flame sheet. In addition, the leads of the thermocouple were aligned along an isotherm (parallel to the flame sheet) to minimize conductive heat losses from the thermocouple bead. A wide range of equivalence ratios has been used in different experiments, from fuel lean mixtures to fuel rich mixtures for angle of nozzles (30, 45, 60 deg.).

Temperature starts to decrease on both sides, rich and lean, because of the chemical mixing of the reactants disproportionately. In addition, it can be observed that the temperature distribution variation depends on the change of nozzle angle. Through figure 12, one can noticed that the place of maximum temperature is related to an angle of the jet due to the perfect mixing between fuel and air that determined by the angle of path reactant. From this work one can see that the location of maximum flame temperature between opposite burners occurs almost at stoichiometric air to fuel ratio ($\varphi = 1$), which is changed with the change of jet angle.

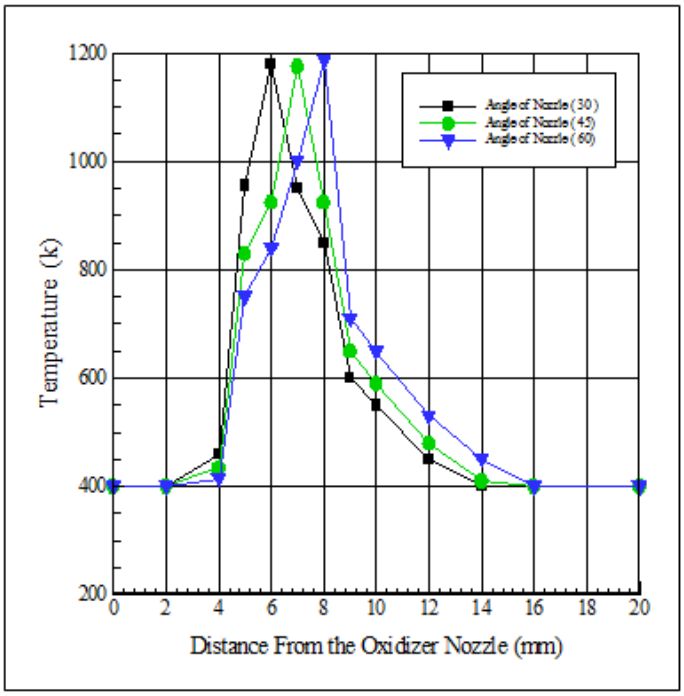

Fig. 12: Effect of jet angles on the location of the counter flame temperature.

V. CONCLUSIONS

Based on a limited amount of experimentation, several conclusions can be made regarding the use of laminar counterflowing jets for combustion research.

1. The velocity measurements reveal that the axial and radial velocity components varied sinusoidally with time.

https://dx.doi.org/10.22161/ijaers/3.10.31 *ISSN: 2349-6495(P) | 2456-1908(O)*

2. The rms of the periodic velocity fluctuations is comparable to, or larger than, the flow bulk velocity suggesting that oscillated flames may withstand, for a limited period of time, instantaneous strain rates larger than those which resulted in extinction of the respective unforced flames.
3. The transition between positive and negative circulation is characterized by a decrease in the jet diameter upstream of the vortex and an even larger increase in the instantaneous strain rate.
4. If the duration of the oscillation was smaller than a critical extinction time scale, extinction did not occur and quenching of the reaction was due to the gradual weakening of the flame over several cycles, during which the temperature was reduced.
5. Mixing between the two forced opposed streams of different reactant compositions was enhanced with lean versus rich flames.
6. Getting the maximum flame temperature when the equivalent ratio (Φ = 1.02) for three types of nozzle (30, 45, 60 deg.) at the constant diameter of jet burner (d = 12 mm).
7. Flame front disc in counterflow burner depends on the design burner and location of honeycomb, screen and bolls.
8. Diameter of disc flame front in the counterflow burner increases with the nozzle angle decrease.

ACKNOWLEDGMENTS

The author would like to thank and acknowledge the staff of workshop in Sulaimani Polytechnic University-Engineering Technical Collage for helping to construct the test rig.

REFERENCES

[1] Chelliah, H. K., and Williams, F. A., Twenty-Third Symposium (International) on Combustion, the combustion Institute, Pittsburg, p. 503, 1990.

[2] Mounaim, C., and Gokalp, I., "Spring meeting of the Western States of the Combustion Institute, Salt Lake City, Utah, 1993.

[3] Katerina, A. M., and Whitelaw, J. H. "Extinction of turbulent counterflow flames under periodic strain", Combustion and Flame, 120: 265-284, 2000.

[4] Frozakis, C. E., Tomboulides, A. G., Lee, J., and Boulouchos, K., "Diffusion to Premixed flames in an H2/air opposed-jet burner". Combustion and Flame, 130: 171-184, 2002.

[5] Frozakis, C. E., Tomboulides, A. G., Lee, J., and Boulouchos, K., "Transient phenomena during diffusion/ edge flame transitions in an opposed-jet hydrogen/air burner", Proceeding of the Combustion Institute, 29: 1581-1587, 2003.

[6] Andrea, C., "Hydrogen and methane edge and diffusion flames in opposed jet configurations", for the Ph.D. Thesis of technical sciences, Swiss Federal Institute of Technology Zurich, 2006.

[7] Kent, J.H., and Bastin, S.J. Parametric effects on sooting in turbulent acetylene diffusion flames. Combust. Flame, 56, 29, 1984.

[8] Qamar, N.H., Nathan, G.J., Alwahabi, Z.T., and King, K.D. The effect of global mixing on soot volume fraction: measurements in simple jet, precessing jet, and bluff body flames. Proc. Comb. Inst., 30, 1493, 2005.

[9] Law, C. K., Sung, C. J. Yu, G., and Axelbaum, R. L., Combust. Flame 98:139-154, 1994.

[10] Richter, H., and Howard, J.B. Formation of polycyclic aromatic hydrocarbons and their growth to soot- a review of chemical reaction pathways. Progress in Energy and Combustion Science, 26, 565, 2000.

[11] KEE, R.J., MILLER, J. A., and RSOX, T. H.: Sandia National Laboratories Report, SAND80- 8003, 1980.

[12] KEE, R.J., WARNATZ,J., and MILLER,J. A., Sandia National Laboratories Report, SAND83-8209. 1983.

[13] KATERINA SARDI, TAYLOR, A. M. K. P., and WHITELAW, J. H. Extinction of Turbulent Counterflow Flames under Periodic Strain COMBUSTION AND FLAME 120:265–284, 2000.

[14] Jassim, M. The Effects of Nozzle Angle and Distance Between Burners on Burning Velocity in Counter Flames, International Journal of Scientific & Engineering Research, Volume 6, Issue 9, September-2015.

[15] Hamins, A., Thridandam, H., and Seshadri, K., Chemical Engineering Science, 40: 2027-2038, 1985.

[16] Puri, I. K., "The structure and extinction of counterflow flames", Ph.D. Thesis, University of California, San Diego. 1987.

[17] Yong, L., Don, J., and Ishwar, K., "Heat release mechanisms in inhibited laminar counterflow flames", Fire, Combustion and Hazardous Waste Processing, ASME vol. 296, 1994.

[18] Egolfopoulos, F. N., Hazardous Waste Processing, ASME, Twenty-Fifth Symposium (International) on Combustion, The Combustion Institute, Pittsburgh, vol. 296 p.1365, 1994.

[19] Sardi, K., and Taylor, A. M. K. P., in The Eleventh Symposium on Turbulent Shear Flows, p. 8–19. 1997.

[20] Karagozian, A. K., and Marble, F. E., Combust. Sci. Technol. 45:65, 1986.